

Osimertinib (AZD9291) increases radio-sensitivity in EGFR T790M non-small cell lung cancer

NANNAN WANG^{1-3*}, LINLIN WANG^{2*}, XIANGJIAO MENG², JIA WANG⁴,
LIFANG ZHU⁴, CHANGTING LIU⁴, SHAORONG LI⁴, LI ZHENG⁴,
ZHENFAN YANG⁴, LIGANG XING² and JINMING YU^{2,1}

¹Department of Oncology, School of Medicine and Life Sciences, University of Jinan-Shandong Academy of Medical Sciences, Jinan, Shandong 250022; ²Department of Radiation Oncology, Shandong Key Laboratory of Radiation Oncology, Shandong Cancer Hospital Affiliated to Shandong University, Shandong Academy of Medical Science, Jinan, Shandong 250117; ³Department of Radiation Oncology, Qingdao University Medical College Affiliated Yantai Yuhuangding Hospital, Yantai, Shandong 264000; ⁴Asia Innovative Medicines and Early Development, AstraZeneca, Shanghai 201203, P.R. China

Received February 28, 2018; Accepted October 8, 2018

DOI: 10.3892/or.2018.6803

Abstract. Osimertinib (AZD9291) is a third generation epidermal growth factor receptor (EGFR) tyrosine kinase inhibitor that has demonstrated significant clinical benefits in patients with EGFR-sensitizing mutations or the T790M mutation. However, the potential therapeutic effect of osimertinib combined with ionizing irradiation (IR) is not well understood. The present study investigated treatment with osimertinib combined with IR in EGFR T790M non-small cell lung cancer (NCI-H1975) *in vitro* and *in vivo*. The results revealed that osimertinib inhibited proliferation and clonogenic survival following irradiation, decreased G2/M phase arrest in irradiated cells, and delayed DNA damage repair in a concentration- and time-dependent manner. Furthermore, osimertinib alone or in combination with IR, blocked the phosphorylation of EGFR (Tyr1068/Tyr1173), protein kinase B and extracellular signal-regulated kinase. Osimertinib also enhanced the antitumor activity of IR in tumor-bearing nude mice. The results of the present study indicated that osimertinib has therapeutic potential as a radiation-sensitizer in lung cancer cells harboring the

EGFR T790M mutation, providing a rationale for clinically combining osimertinib with irradiation in EGFR T790M non-small cell lung cancer.

Introduction

Lung cancer is the leading cause of cancer-associated mortality worldwide, and non-small cell lung cancer (NSCLC) accounts for 80-85% all lung cancer cases (1). Tumors harboring somatic activating mutations in the exon encoding the kinase domain of epidermal growth factor receptor (EGFR), account for 10-15% (2,3) and 40% (4) of NSCLC cases in the Western and Asian populations, respectively. EGFR tyrosine kinase inhibitors (TKIs) present a novel paradigm for molecular targeted therapeutics for patients with NSCLC and are recommended as first-line treatments for patients with advanced NSCLC harboring an EGFR-TKI-sensitizing mutation (EGFRm) (5,6). Despite reports of high response rates with first-line EGFR-TKI therapy, the majority of responsive patients ultimately develop disease progression following 9-14 months of treatment, and ~50% cases are caused by the acquisition of the T790M mutation (7-9). Osimertinib (TAGRISSO™, AZD9291) is an oral, irreversible, third generation EGFR-TKI that targets EGFRm and T790M (10,11). It has been approved by the US Food and Drug Administration for the management of T790M-positive NSCLC that has progressed following the introduction of first-line EGFR-TKI treatment (12). Furthermore, a recently published study (FLAURA) demonstrated that osimertinib as a first-line treatment for patients with EGFRm and locally advanced or metastatic NSCLC, significantly extended progression-free survival when compared with patients treated with first generation EGFR-TKIs (18.9 vs. 10.2 months) (13).

Radiotherapy is an important treatment modality for lung cancer, particularly for patients who are ineligible for surgery. Approximately 2/3 of patients with lung cancer receive

Correspondence to: Professor Ligang Xing or Professor Jinming Yu, Department of Radiation Oncology, Shandong Key Laboratory of Radiation Oncology, Shandong Cancer Hospital Affiliated to Shandong University, Shandong Academy of Medical Science, 440 Jiyan Road, Jinan, Shandong 250117, P.R. China
E-mail: xinglg@medmail.com.cn
E-mail: sdyujinming@163.com

*Contributed equally

Key words: non-small cell lung cancer, epidermal growth factor receptor, T790M mutation, osimertinib, ionizing radiation

radiotherapy during the course of treatment, with either definitive or palliative intent (14). However, the effectiveness of radiotherapy is often limited by intrinsic radio-resistance. The expression and activity of EGFR are determinants of the radioresponse in patients with NSCLC, and anti-EGFR therapy has been shown to enhance the radiosensitivity of tumor cells (15-17). Recent data demonstrated that patients with EGFR mutations have improved outcomes when treated with a combination of first-generation EGFR-TKIs and radiotherapy (18-21). However, to the best of our knowledge, no previous studies have discussed the effectiveness of osimertinib combined with ionizing radiation (IR).

In the present study, the effects of osimertinib on the radiosensitivity of NSCLC cells with T790M/L858R mutations were evaluated *in vitro* and *in vivo*.

Materials and methods

Cell lines and reagents. The human lung cancer cell line, NCI-H1975 (L858R/T790M), was obtained from the American Type Culture Collection (Manassas, VA, USA) and authenticated by short-tandem repeat analysis in December 2016. The cells were maintained in RPMI-1640 (cat. no. 22400; Invitrogen; Thermo Fisher Scientific, Inc., Waltham, MA, USA), containing 10% fetal bovine serum (Hyclone; GE Healthcare Life Sciences, Logan, UT, USA; cat. no. SV30087) in a humidified incubator at 37°C with 5% CO₂. Osimertinib (AZD9291) was provided by AstraZeneca (Shanghai, China), and was dissolved in dimethyl sulfoxide (DMSO; Sigma-Aldrich; Merck KGaA, Darmstadt, Germany; cat. no. SHBG6226v) for *in vitro* study and 0.5% Hydroxy propyl methyl cellulose (HPMC; Sigma-Aldrich; Merck KGaA; cat. no. 9004-67-5)/0.1% Tween-80 (cat. no. P1754; Sigma-Aldrich; Merck KGaA) for the *in vivo* study.

Irradiation. The cells and xenografts were irradiated using the X-cell 160 Irradiator (¹³⁷Cs; Kubtec, Milford, CT, USA) at a dose rate of 140 cGy/min at room temperature with the following protocol: 1.42 min at 2 Gy, 2.85 min at 4 Gy, 4.26 min at 6 Gy, 5.68 min at 8 Gy, 7.10 min at 10 Gy and 14.2 min at 20 Gy, respectively. Cells were treated with Osimertinib at 37°C 1 h prior to irradiation in the combination groups involved in the *in vitro* study.

In vitro cell proliferation assays [3-(4,5-dimethylthiazol-2-yl)-5-(3-carboxymethoxyphenyl)-2-(4-sulfophenyl)-2H-tetrazolium, inner salt (MTS) assay]. Cells were divided into 6 groups: i) Osimertinib alone [at dosages of 0 (control), 0.0001, 0.001, 0.003, 0.01, 0.03, 0.1, 0.3, 1 and 3 μM, respectively]; ii) osimertinib with 2 Gy irradiation; iii) osimertinib with 4 Gy irradiation; iv) osimertinib with 6 Gy irradiation; v) osimertinib with 8 Gy irradiation; and vi) osimertinib with 10 Gy irradiation. The proliferation analysis was performed using a tetrazolium-based Cell Titer 96® Aqueous One Solution Assay (cat. no. G3581; Promega Corporation, Madison, WI, USA), according to the manufacturer's instructions. Briefly, exponentially growing cells were diluted to 2x10⁴/ml and seeded at 100 μl/well into 96-well plates. Following 24 h, cells were treated with irradiation and increasing concentrations of osimertinib. Then, an MTS assay was performed following

3 days. Relative cell viability was expressed as the percentage of untreated control.

In vitro cell clone formation assay (CFA). Cells in the log phase were plated into 6-well plates with the desired cell density (300 cells/well for 0 Gy, 500 cells/well for 2 Gy, 1,000 cells/well for 4 Gy, 3,000 cells/well for 6 Gy and 5,000 cells/well for 8 Gy, respectively) and pretreated with osimertinib at 10, 30 and 100 nM, or DMSO, respectively. Irradiation was delivered 1 h later. Cells were then maintained for 14 days with osimertinib in RPMI-1640 and stained with 0.1% crystal violet (Sigma-Aldrich; Merck KGaA; cat. no. 5K219R5). Colonies of >50 cells were defined as surviving colonies and the number of colonies was normalized to that of non-irradiated controls. The sensitizer enhancement ratio (SER) for osimertinib treatment was calculated as the ratio of the mean inactivation dose of control cells / the mean inactivation dose of osimertinib-treated cells at the 0.01 survival fraction.

Flow assisted cell sorting (FACS) assay. Cells were trypsinized with 0.25% trypsin-EDTA (cat. no. 25200-114; Invitrogen; Thermo Fisher Scientific, Inc.) and the suspended cell pellet was incubated with 70% ethanol (cat. no. 1000927; Sinopharm Chemical Reagent Co., Ltd., Shanghai, China) at 4°C. Following the thorough removal of ethanol, the cells were suspended in a propidium iodide (PI) staining solution (cat. no. P3566; Invitrogen; Thermo Fisher Scientific, Inc.) in the dark, at room temperature for 30 min. Flow cytometry was performed using a FACSCanto Cell Analyzer (V07300617; BD Biosciences, Franklin Lakes, NJ, USA).

Immunofluorescence assay. Cells were cultured on chamber slides and the samples were collected at 2, 24 and 48 h, respectively. Cells were washed with ice-cold Ca²⁺/Mg²⁺-free phosphate buffered saline (PBS), and fixed in 4% formaldehyde (cat. no. SZBF0690v; Sigma-Aldrich; Merck KGaA) for 60 min at room temperature. Following permeabilization in 1% Triton X-100 (cat. no. 057K00161; Sigma-Aldrich; Merck KGaA) and blocking with 5% bovine serum albumin (BSA; cat. no. 12575v; Sigma Aldrich; Merck KGaA)/0.3% Triton™ X-100 in PBS at room temperature for 1 h, the cells were incubated with a fluorescein isothiocyanate-conjugated anti-phospho histone γ-H2A histone family member X (H2AX) primary antibody (dilution, 1:800; cat. no. 2577s; CST Biological Reagents Co., Ltd., Shanghai, China) overnight at 4°C, then incubated with an Alexa 647-conjugated anti-rabbit secondary antibody (dilution, 1:1,000; cat. no. 4412S; CST Biological Reagents Co., Ltd.) for 1 h at room temperature in the dark. Coverslips were mounted using Mounting Medium with DAPI (H-1200; Vector Laboratories, Inc., Burlingame, CA, USA) overnight at 4°C. Images were acquired with an Olympus BX61 laser scanning confocal microscope (7E18988; Olympus Corporation, Tokyo, Japan) using x60 magnification. Using ≥150 cells from each experiment, the cells were counted and the percentage of cells positive for γ-H2AX was calculated. A positive cell was defined by >5 discrete dots in the nucleus.

Western blotting. Cells were lysed in 2X SDS buffer containing protease and phosphatase inhibitors (cat. no. 1861282; Thermo

Fisher Scientific, Inc.), then the protein concentration was determined via a BCA protein assay (cat. no. 34076; Thermo Fisher Scientific, Inc.). Equal amounts of protein (20 μ g/well) were loaded for SDS-PAGE using 4-12%-gradient Bis-Tris precast gels (cat. no. 345-0124; Bio-Rad Laboratories, Inc., Hercules, CA, USA), followed by transfer to polyvinylidene difluoride membranes using the iBlot dry transfer system (cat. no. IB21001; Novex; Thermo Fisher Scientific, Inc.). Membranes were blocked in 5% fat-free milk in Tris-buffered saline with 0.1% Tween-20 (TBS-T) for 30 min at room temperature, then incubated at 4°C overnight with the following primary antibodies: Total EGFR (dilution, 1:1,000; cat. no. 4267S; CST Biological Reagents Co., Ltd.), phospho (p)-EGFR (dilution, 1:1,000; Tyr1068, cat. no. 3777S; or Tyr1173, cat. no. 4407S; CST Biological Reagents Co., Ltd.), total protein kinase B (AKT; dilution, 1:1,000; cat. no. 4691S; CST Biological Reagents Co., Ltd.), phospho-AKT (Ser473; dilution, 1:1,000; cat. no. 12694S; CST Biological Reagents Co., Ltd.), total extracellular signal-regulated kinase (ERK; dilution, 1:1,000; cat. no. 4695S; CST Biological Reagents Co., Ltd.), phospho-ERK (dilution, 1:1,000; Thr202/Tyr204; cat. no. 4370S; CST Biological Reagents Co., Ltd.) and GAPDH (dilution, 1:10,000; cat. no. 2118L; CST Biological Reagents Co., Ltd.). Membranes were then incubated for 1 h at room temperature with a horseradish peroxidase (HRP)-conjugated secondary antibody (dilution, 1:2,000; cat. no. 7074 or 7076; CST Biological Reagents Co., Ltd.). Membranes were visualized using a mixed detection solution (Super Signal West Dura Extended Duration Substrate; cat. no. 34076; Thermo Fisher Scientific, Inc.) for 5 min at room temperature, protected from light. Densitometry of western blots was conducted using a Fujifilm Image Reader LAS-4000 2.1 (Fujifilm Corp., Tokyo, Japan).

Mice and tumor model. Specific pathogen-free immunodeficient female nude mice (n=170; age, 6-8 weeks; weight, 20-25 g) were purchased from Beijing Vital River Laboratory Animal Technology (Beijing, China). Animals had free access to food and water, and were maintained at 21-23°C with 40-70% humidity and a 12-h light/dark cycle. All of the animal studies were approved by the Institutional Animal Care and Use Committee of AstraZeneca (Shanghai, China). NCI-H1975 tumor cells (5×10^6 cells/0.1 ml) were injected subcutaneously into the left flank of the nude mice to establish the tumor model.

In vivo efficacy study. Tumor growth was monitored twice weekly by caliper measurements. When the tumors grew to 0.2-0.4 cm³, the mice were randomized into 6 groups: i) vehicle (no treatment); ii) osimertinib alone (5 mg/kg/day); iii) 2 Gy x 10 F irradiation alone (5 fractions/week from the first day); iv) 2 Gy x 10 F irradiation and osimertinib (5 mg/kg/day); v) 20 Gy x 1 F irradiation alone on the first day; and vi) 20 Gy x 1 F irradiation and osimertinib (5 mg/kg/day). Osimertinib was administered at 5 mg/kg once daily by oral gavage for 31 days. Mice were euthanatized (by excessive CO₂ inhalation) 25 days following the termination of osimertinib treatment to evaluate the persistent inhibitory effect, or when tumor volume $\geq 1,500$ mm³ according to the Animal Welfare of the Institutional Animal Care and Use Committee of

AstraZeneca (10). Power analysis was performed whereby group sizes were calculated to enable statistically robust detection of tumor growth inhibition. Tumor growth inhibition from the start of treatment was assessed by comparing the mean change in tumor volume of the control and treatment groups.

In vivo drug metabolism and pharmacokinetics (DMPK/PD) assay. For pharmacodynamic studies, mice were randomized when the tumor volumes reached 0.5-0.8 cm³. Mice were treated with either a single dose of osimertinib, IR alone (20 Gy x 1 F), or osimertinib plus IR. Following a single dose, the blood plasma was collected, except for that of the IR 20 Gy x 1 F group due to the absence of osimertinib in the plasma, and the tumors of all groups were harvested 0, 0.5, 1, 2, 4, 7, 16 and 24 h later. The total osimertinib concentration in plasma was detected using the ACQUITY SM Method, as previously described (22). Sections were fixed with 4% formalin for 24 h at room temperature, embedded in paraffin and were then immunohistochemically stained for the phosphorylated forms of EGFR (Tyr1068) and EGFR (Tyr1173).

Immunohistochemistry (IHC). IHC was performed on 3- μ m sections using a Lab Vision autostainer. The tumors were excised as aforementioned for the DMPK/PD assay. The paraffin slides were incubated at 56°C for 30 min then dewaxed and rehydrated in a Leica Autostainer XL and subjected to antigen retrieval (cat. no. S1699; Dako; Agilent Technologies, Inc., Santa Clara, CA, USA) for 15 min at room temperature followed by washing under running tap water for 5 min. Then the sections were rinsed in TBS-T, and assessed on a LabVision autostainer. Following incubation with an endogenous peroxidase blocker (3% hydrogen peroxide; cat. no. GTX30967; GeneTex, Inc., Irvine, CA, USA) for 10 min at room temperature, slides were washed twice in TBS-T and blocked with 5% BSA (cat. no. 12575v; Sigma Aldrich; Merck KGaA) at room temperature for 10 min. Sections were then incubated with the following primary antibodies for 60 min at room temperature: p-EGFR Tyr1068 (dilution, 1:200; cat. no. 2234; CST Biological Reagents Co., Ltd.), p-EGFR Tyr1173 (dilution, 1:200; cat. no. 4407; CST Biological Reagents Co., Ltd.), Histone H2AX phospho (ser139; dilution, 1:150; cat. no. 2577; CST Biological Reagents Co., Ltd.) and cleaved caspase-3 (CC3) (Asp175; dilution, 1:200; cat. no. 9661; CST Biological Reagents Co., Ltd.). The sections were then washed twice in TBS-T. The p-EGFR (Tyr1068/Tyr1073)/CC3 slides were incubated with a biotinylated goat anti-rabbit immunoglobulin secondary antibody (cat. no. E0432; dilution, 1:100; Dako; Agilent Technologies, Inc.) and Streptavidin-Peroxidase for 30 min at room temperature. The Histone H2AX phospho slides were incubated with EnVision system-HRP Labeled Polymer Anti-Rabbit for 30 min at room temperature and washed twice in TBS-T. All sections were incubated in diaminobenzidine substrate for 5 min at room temperature and rinsed with tap water. The sections were then counter stained with Mayer's hematoxylin for 5 min at room temperature, dehydrated and cleared with xylene in a Leica XL autostainer, and finally sealed in the ClearVue automated cover slipper. Images were acquired with a laser scanning confocal microscope (Olympus BX61 microscope; Olympus Corporation).

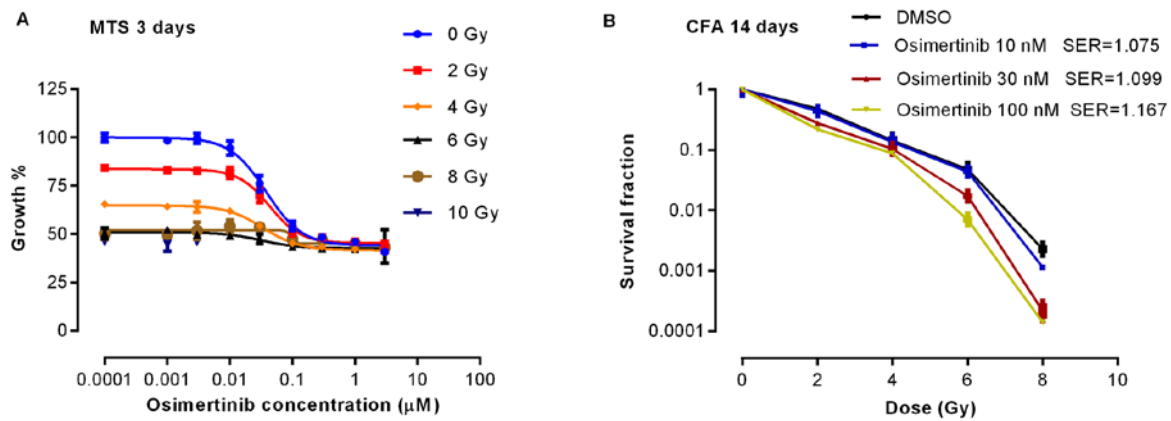


Figure 1. Osimertinib inhibits cell proliferation. Cells were treated with osimertinib 1 h prior to irradiation, and the cell viability was determined by (A) MTS assay following 3 days of treatment, and (B) CFA following 14 days of treatment. The experiments were repeated 3 times. Data are presented as the mean \pm standard error of the mean. MTS, 3-(4,5-dimethylthiazol-2-yl)-5-(3-carboxymethoxyphenyl)-2-(4-sulfophenyl)-2H-tetrazolium, inner salt; CFA, clone fraction assay; DMSO, dimethyl sulfoxide; SER, sensitizer enhancement ratio.

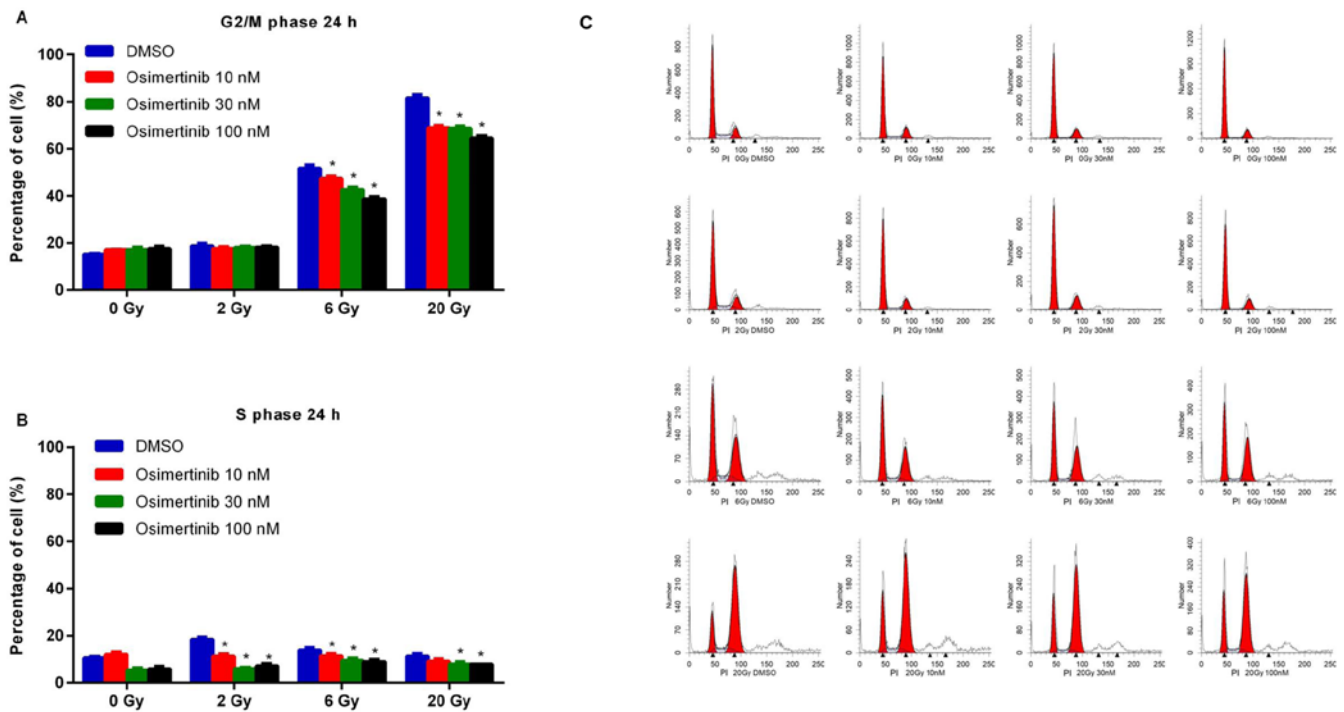


Figure 2. Cell cycle redistribution following treatment. Cells were treated with osimertinib 1 h prior to IR. Following 24 h post-IR, cell cycle changes were analyzed by flow cytometry: (A) G2/M phase and (B) S phase. (C) Representative cell cycle distributions among the different groups. * $P < 0.05$ vs. IR alone. IR, irradiation; DMSO, dimethyl sulfoxide.

Statistical analysis. Experiments were performed ≥ 3 times and data are presented as the mean \pm standard error of the mean. Statistical analysis was performed using SPSS 19.0 (IBM Corp., Armonk, NY, USA). One-way analysis of variance (ANOVA) with a Bonferroni post hoc test were conducted for comparisons of the percentage of H2AX positive cells in the immunofluorescence assay, percentage of cells in S and G2/M phase in the flow cytometry assay, the tumor volume 25 days following the final day of osimertinib treatment and the quantitative changes of protein phosphorylation in the western blotting and IHC. Two-way ANOVA with a Bonferroni post hoc test was applied for the comparison of tumor volume in the tumor growth curves. Pearson coefficient-parametric

analysis was performed to determine whether there was a correlation between the phosphorylated forms of EGFR (Tyr1068/Tyr1173) and the concentration of osimertinib in the blood plasma. $P < 0.05$ was considered to indicate a statistically significant difference.

Results

Osimertinib promotes the inhibition of cell proliferation in NSCLC following irradiation. To determine the effect of osimertinib combined with irradiation on cell proliferation, the present study performed a cell viability assay 3 days following treatment. As shown in Fig. 1A, the rate of cell proliferation

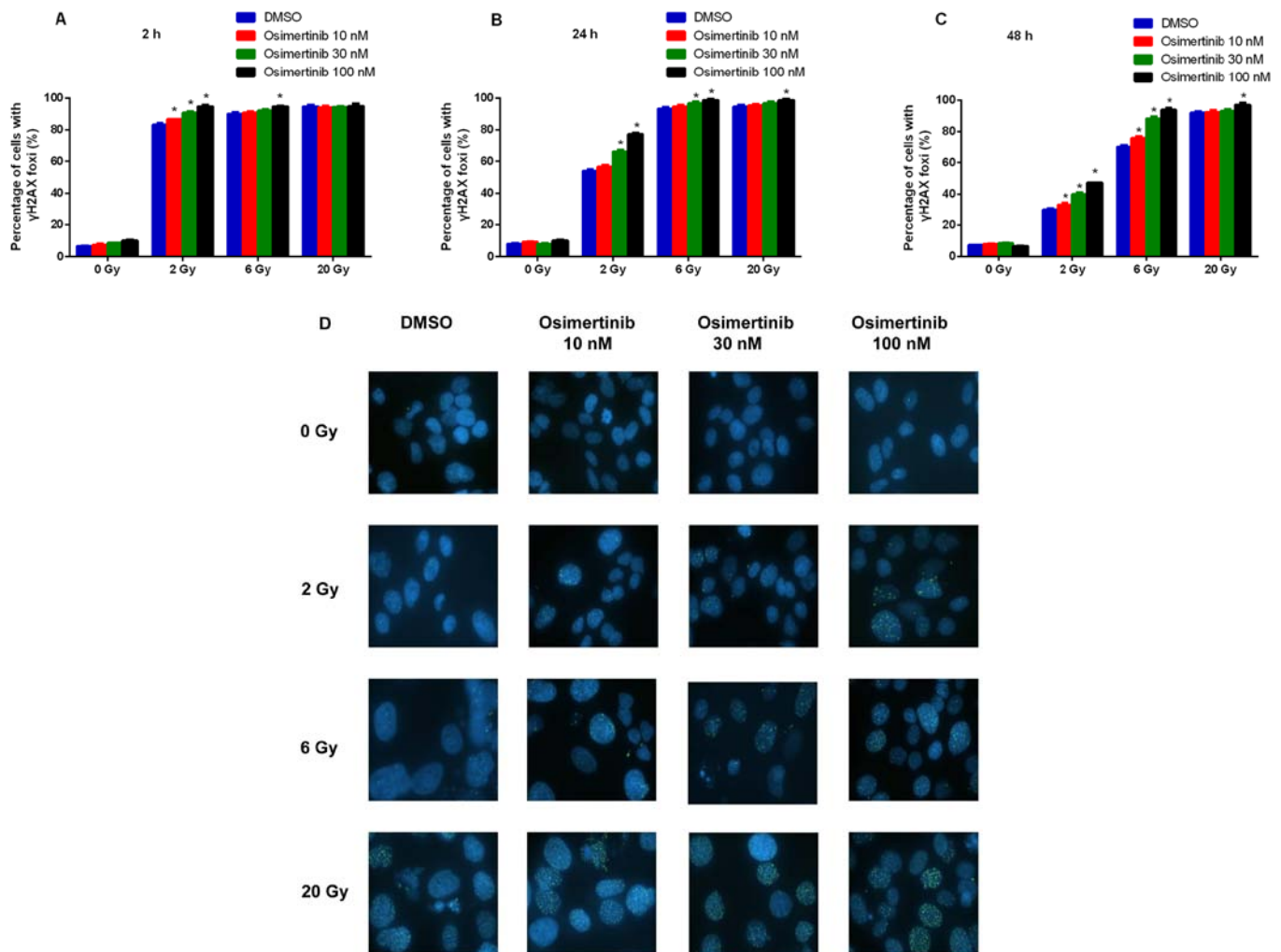


Figure 3. Osimertinib causes a delay in DNA damage repair in NCI-H1975 cells. The change in the proportion of cells with positive γ -H2AX foci (A) 2, (B) 24 and (C) 48 h following treatment. (D) Representative images of γ -H2AX foci 48 h following treatment (magnification, x60). * $P < 0.05$ vs. IR alone. IR, irradiation; DMSO, dimethyl sulfoxide; γ -H2AX, H2A histone family member X.

decreased markedly when osimertinib was administered prior to 2 or 4 Gy irradiation. Proliferation was demonstrated to be inhibited in a dose-dependent manner by CFA in which the SER was >1 , indicating that the effect on proliferation inhibition was synergistic when irradiation was combined with osimertinib treatment (Fig. 1B).

Osimertinib reduces G2/M-phase cell cycle arrest following irradiation. To assess the effects of osimertinib on cell cycle arrest following irradiation, cells were treated with 10, 30 or 100 nM osimertinib for 24 h and then irradiated with dose of 2, 6 or 20 Gy due to their different role in clinical practice: 2 Gy was recognized as the conventional fraction; 6 Gy was chosen due to the best inhibiting effect as determined by CFA in Fig. 1; and 20 Gy represented hypofractionated radiotherapy. As shown in Fig. 2, dose-dependent reductions in the G2/M and S phases were demonstrated in the combination treatment group when compared with irradiation alone (DMSO group).

Osimertinib inhibits IR-induced DNA double-strand breaks (DSB) repair in NCI-H1975 cells. To determine whether the increased radio-sensitivity of cell lines following osimertinib

treatment was a product of compromised DNA-break repair, the present study conducted immunofluorescence staining for γ -H2AX in NCI-H1975 cells. It was revealed that the formation of γ -H2AX began to increase in the 2 and 6 Gy groups at 2 (Fig. 3A) and 24 h (Fig. 3B); whilst the formation of γ -H2AX only began to increase at 24 h in the 20 Gy group (Fig. 3C). In addition, osimertinib significantly increased the number of γ -H2AX foci per cell at 48 h following 2 and 6 Gy radiation in a dose-dependent manner (Fig. 3C and D).

Osimertinib reduces the phosphorylation of EGFR involved in the AKT/ERK signaling pathway following IR. Osimertinib was revealed to be a potent inhibitor of EGFR and downstream signaling substrate (p-AKT and p-ERK) phosphorylation in cells with mutant EGFR (10). Therefore, the present study investigated whether AKT/ERK were the main downstream targets of EGFR proteins following treatment with osimertinib combined with radiation. The western blotting results demonstrated that osimertinib inhibits p-EGFR (1068)/p-EGFR (1173)/p-AKT/p-ERK protein expression when treated alone or in combination with IR in a concentration-dependent manner (Fig. 4).

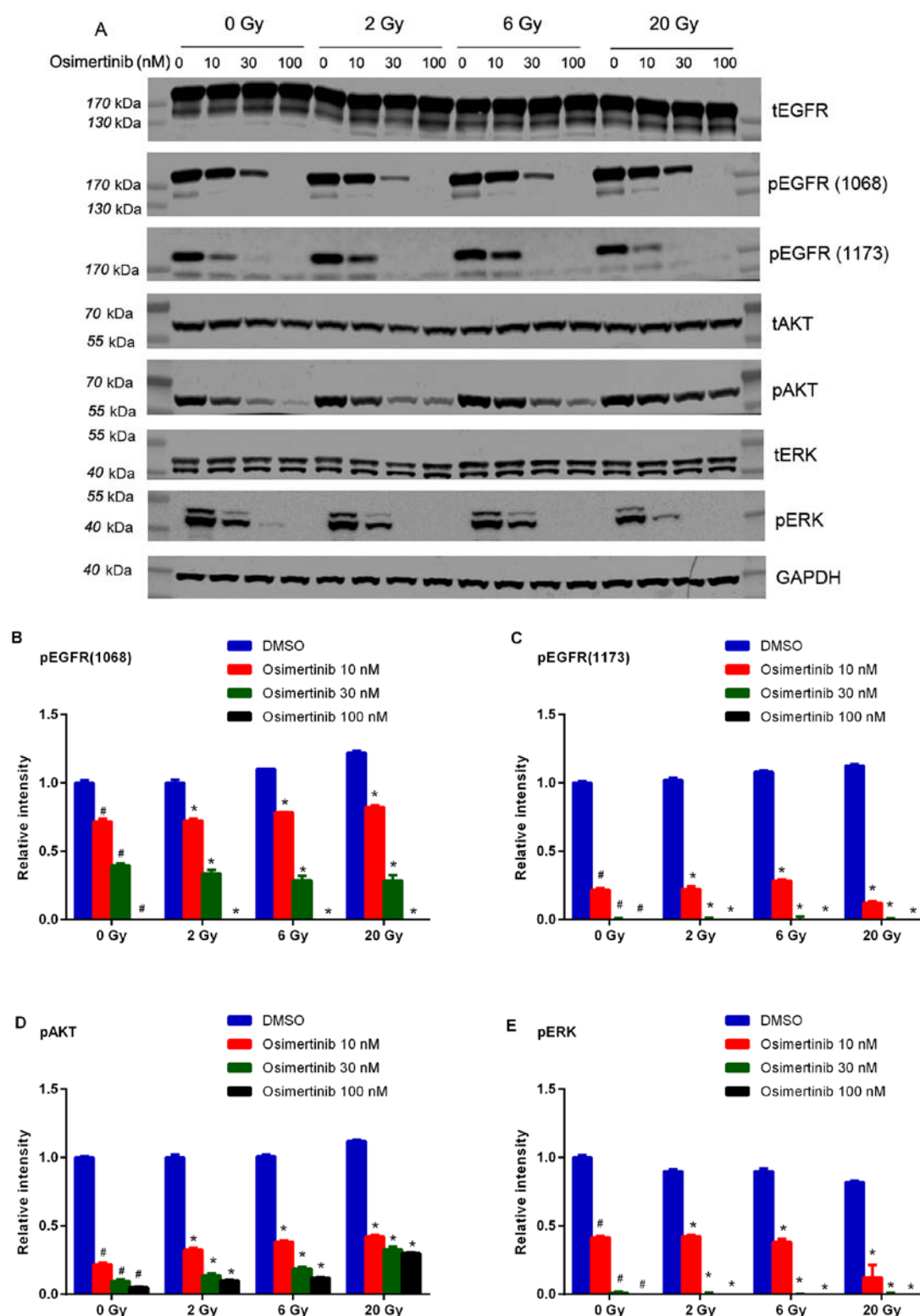


Figure 4. Western blot analysis of the effect of osimertinib combined with IR on EGFR phosphorylation levels *in vitro*. Cells were treated with osimertinib 1 h prior to IR, and cell proteins were collected 2 h following IR treatments. GAPDH was included as a loading control. (A) Western blot analysis. (B-E) Quantitative analysis of changes in (B) p-EGFR (1068), (C) p-EGFR (1173), (D) p-AKT and (E) p-ERK, respectively. *P < 0.05 vs. IR alone; #P < 0.05 vs. DMSO control. IR, irradiation; DMSO, dimethyl sulfoxide; p-, phosphorylated; EGFR, epidermal growth factor receptor; AKT, protein kinase B; ERK, extracellular signal-regulated kinase.

Osimertinib combined with IR induces tumor regression in the NCI-H1975 xenograft model. To explore the *in vivo* activity of osimertinib combined with IR, the present study administered osimertinib during the irradiation of nude mice

bearing NCI-H1975 subcutaneous xenografts. As shown in Fig. 5A, the combination treatment exhibited more potent antitumor efficacy when compared with IR or osimertinib alone. At the end of the treatments, the mean residual tumor

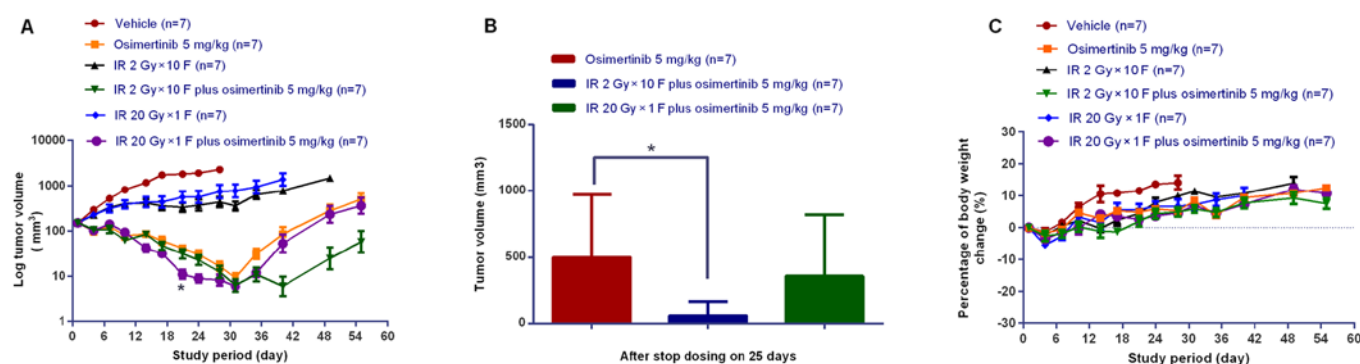


Figure 5. Antitumor efficacy of osimertinib combined with IR in the NCI-H1975 xenograft models. (A) Tumor growth curves. * $P < 0.05$ vs. IR alone. (B) Tumor volume 25 days following the final day of treatment. * $P < 0.05$, as indicated. (C) Changes in body weight over the study period. IR, irradiation.

volume in the IR 2 Gy x 10 F plus osimertinib 5 mg/kg group was lower than that of osimertinib alone or osimertinib plus IR 20 Gy x 1 F groups (Fig. 5A and B). In addition, the tumor complete response rates were 1/7, 3/7 or 4/7 for the osimertinib alone, osimertinib plus IR 20 Gy x 1 F or osimertinib plus IR 2 Gy x 10 F groups, respectively, at the time of treatment termination (day 31). Inhibition of tumor growth was observed for an additional 25 days following treatment termination (Fig. 5A and B). It was demonstrated that radiation of conventional fraction may be more powerful than hypofractionated radiotherapy when combined with osimertinib administration; however, this requires further investigation in future clinical observations. The present study also measured mouse body weight in order to assess the treatment tolerability, and no evident body weight changes were observed ($<5\%$ of starting body weight), as shown in Fig. 5C. These results suggested that treatment with IR combined with osimertinib was tolerated well.

DMPK/PD correlation and osimertinib target-inhibition confirmation in combination with IR in NCI-H1975 subcutaneous xenograft models. To confirm the target and pathway of osimertinib activity when in combination with IR, the present study examined the total osimertinib concentration in the plasma and the phosphorylation level of EGFR in tumor tissues following treatments. In the osimertinib and osimertinib plus IR groups, the expression of p-EGFR (Tyr1068)/p-EGFR (Tyr1173) was negatively associated with the plasma concentration of osimertinib (Fig. 6A and B). As displayed by the representative IHC quantification of p-EGFR (Tyr1068)/p-EGFR (Tyr1173)/ γ -H2AX and cleaved caspase-3 (Fig. 6C-G), osimertinib suppressed the activity of p-EGFR (Tyr1068)/p-EGFR (Tyr1173), particularly when administrated combined with IR; while the phosphorylation of EGFR maintained high levels in the IR only group. However, the expression levels of γ -H2AX and cleaved caspase-3 significantly increased in the osimertinib plus IR combination group.

Discussion

Osimertinib is an irreversible third generation EGFR-TKI that has demonstrated significant potency in patients with NSCLC with EGFR-sensitizing mutations and the T790M-resistance mutation (10). First generation EGFR-TKI therapy coupled

with radiotherapy was revealed to have the potential to improve outcomes for patients with NSCLC exhibiting EGFR-sensitive mutations (9,23-25). However, the role of osimertinib in the effect of IR remains elusive. In the present study, it was demonstrated that osimertinib combined with IR could significantly decrease the proliferation of NSCLC cells harboring the T790M/L858R mutation *in vitro* and *in vivo*, reduce G2/M-phase cell cycle arrest and block IR-induced DNA DSB repair, demonstrating its role in radio-sensitivity. This may provide a rationale for clinically combining osimertinib with IR to treat patients with NSCLC exhibiting EGFR mutations.

Synergistic inhibition of cell proliferation has been reported to be the predominant mechanism underlying the effectiveness of the combination treatment of IR and gefitinib (26,27). In the present study, proliferation and clone formation were significantly inhibited when treated with osimertinib and IR. This antitumor effect was further confirmed in xenograft models. Following the completion of treatment, inhibition of tumor growth was observed for an additional 25 days. This may be indicative of the durable cellular suppression of osimertinib when combined with radiation. However, the optimal combination pattern of osimertinib and IR, such as the fractionated dose, the fractionated number, the timing of osimertinib administration and so on, has not been clear until now. It has been reported that the autophosphorylation of EGFR could be activated following radiation and serves an important role in leading to radiation resistance (28,29). Thus, osimertinib was administrated prior to radiation in the present study. Notably, cell proliferation was inhibited by treatment with osimertinib combined with radiation with the SER >1 , which demonstrated the inhibition of proliferation was at least partly associated with the radio-sensitivity induced by osimertinib. However, the underlying mechanisms still require further investigations.

Radio-sensitization is a consequence of the repair of DNA DSBs mediated through a blockade in EGFR-signaling events (30,31). It has been reported that irradiation can directly activate EGFR signaling to in turn activate DNA DSB repair (28-29,32). A number of processes in the DNA damage response are central to radio-sensitivity, including checkpoint activation and repair (33,34). G2/M-phase-arrest allows cells to repair damaged DNA and can cause IR-resistance. γ -H2AX is thought to be a reporter of tumor radio-sensitivity, induced by IR at DNA DSB sites (35,36). In the present study it was

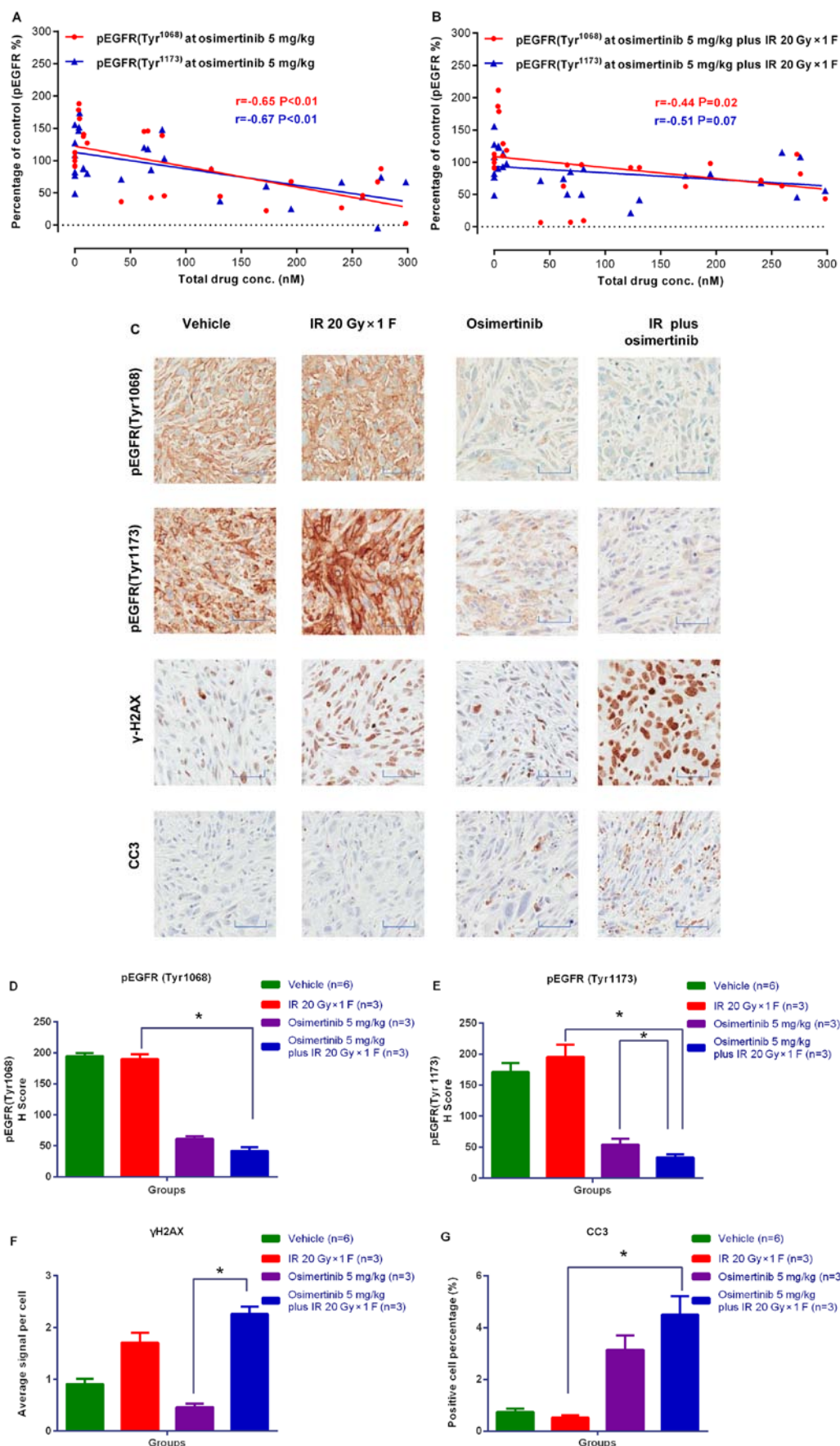


Figure 6. Association between drug metabolism and pharmacokinetics in the NCI-H1975 xenograft model. (A and B) The association between osimertinib concentration in plasma and p-EGFR (Tyr1068)/p-EGFR (Tyr1173) levels in tumor tissues, for (A) osimertinib alone or (B) in combination with IR. (C) The representative immunohistochemical images of p-EGFR (Tyr1068), p-EGFR (Tyr1173), γH2AX and CC3. Scale bars, 100 μm. (D-G) Quantitative analysis of the expression levels of (D) p-EGFR (Tyr1068), (E) p-EGFR (Tyr1173), (F) γH2AX and (G) CC3, respectively. * $P < 0.05$, as indicated. p-, phosphorylated; EGFR, epidermal growth factor receptor; γH2AX, H2A histone family member X; CC3, cleaved caspase-3.

revealed that osimertinib decreased IR-induced G2/M-phase arrest in a dose-dependent manner, and that the level of γ -H2AX in the combination treatment group was increased when compared with that of IR alone. These results may suggest that, when combined with osimertinib, IR shortens G2/M-phase arrest and inhibition of DNA damage repair.

It has been reported that receptor tyrosine kinases and AKT signaling may be activated by IR in NSCLC cells (37-39). AKT is involved in the regulation of cell cycle progression. Third generation agents can induce a switch to multiple signaling mechanisms such as the ERK and AKT signaling pathways, thereby bypassing EGFR-dependency (40-42). In the present study, the slight increase in p-EGFR (1068), p-EGFR (1173) and p-AKT following irradiation was observed, but not for p-ERK. Notably, osimertinib treatment significantly inhibited p-EGFR, p-AKT and p-ERK protein expression alone or in combination with IR *in vitro*; it also significantly decreased the phosphorylation of EGFR *in vivo*. Furthermore, the combination treatment was revealed to increase the rate of apoptosis. This may be another reason for the radio-sensitization role of osimertinib in NSCLC cells exhibiting EGFR mutations. Further investigations are required to determine whether alterations of a specific gene or gene set involved in EGFR expression and apoptosis-associated signaling pathways are modulated by osimertinib.

In conclusion, osimertinib was revealed to enhance the radio-sensitivity of T790M/L858R NSCLC *in vitro* and *in vivo*, suggesting a potential clinical impact for the use of this combination therapeutic strategy. Improved understanding of the molecular mechanisms underpinning the radio-sensitizing effects of osimertinib may enable the development of novel approaches to optimize the treatment of lung cancer.

Acknowledgements

The authors would like to thank Mrs. Minghui Hu (Asia Innovative Medicines and Early Development, AstraZeneca, Shanghai, China) for cell culture assistance, and Mr. Kunji Liu (Asia Innovative Medicines and Early Development, AstraZeneca) for his work on the *in vivo* modeling. They would also like to thank Mrs. Haihua Hu (Asia Innovative Medicines and Early Development, AstraZeneca) for her work on the *in vitro* immunofluorescence assay.

Funding

The present study was supported by grants from the National Health and Family Planning Commission of China (grant no. 201402011), the National Natural Science Foundation of China (grant no. 81472812), the Postdoctoral Innovation of Shandong Province (grant no. 201501010), the Postdoctoral Science Foundation of China (grant no. 2016M590640) and the Innovation Project of the Shandong Academy of Medical Science.

Availability of data and materials

The datasets used and analyzed during the present study are available from the corresponding author upon reasonable request.

Authors' contributions

LW, LX, ZY, LZheng and JY designed the study. NW, JW, LZhu, CL, XM and SL performed the experiments and analyzed the data. NW drafted the manuscript. LW, XM and LX revised the manuscript. All authors reviewed and approved the final manuscript.

Ethics approval and consent to participate

All of the animal studies were approved by the Institutional Animal Care and Use Committee of AstraZeneca (Shanghai, China).

Patient consent for publication

Not applicable.

Competing interests

The authors Mrs. Jia Wang, Mrs. Lifang Zhu, Mrs. Changting Liu, Mrs. Shaorong Li, Mrs. Li Zheng and Mrs. Zhenfan Yang are affiliated with Asia Innovative Medicines and Early Development, AstraZeneca (Shanghai, China). The osimertinib (AZD9291) used in the present study was provided by AstraZeneca.

References

1. Torre LA, Bray F, Siegel RL, Ferlay J, Lortet-Tieulent J and Jemal A: Global cancer statistics, 2012. *CA Cancer J Clin* 65: 87-108, 2015.
2. Reinersman JM, Johnson ML, Riely GJ, Chitale DA, Nicastri AD, Soff GA, Schwartz AG, Sima CS, Ayalew G, Lau C, *et al*: Frequency of EGFR and KRAS mutations in lung adenocarcinomas in African Americans. *J Thorac Oncol* 6: 28-31, 2011.
3. Gahr S, Stoeckl R, Geissinger E, Ficker JH, Brueckl WM, Gschwendtner A, Gattenloehner S, Fuchs FS, Schulz C, Rieker RJ, *et al*: EGFR mutational status in a large series of Caucasian European NSCLC patients: Data from daily practice. *Br J Cancer* 109: 1821-1828, 2013.
4. Shi Y, Au JS, Thongprasert S, Srinivasan S, Tsai CM, Khoa MT, Heeroma K, Itoh Y, Cornelio G and Yang PC: A prospective, molecular epidemiology study of EGFR mutations in Asian patients with advanced non-small-cell lung cancer of adenocarcinoma histology (PIONEER). *J Thorac Oncol* 9: 154-162, 2014.
5. NCCN: NCCN Clinical Practice Guidelines in Oncology NSCLC (version 7.2015), 2015. http://www.nccn.org/professionals/physician_gls/pdf/nscl.pdf. Accessed July 16, 2015.
6. Tan DS, Yom SS, Tsao MS, Pass HI, Kelly K, Peled N, Yung RC, Wistuba II, Yatabe Y, Unger M, *et al*: The International Association for the Study of Lung Cancer consensus statement on optimizing management of EGFR mutation-positive non-small cell lung cancer: Status in 2016. *J Thorac Oncol* 11: 946-963, 2016.
7. Yu HA, Arcila ME, Rekhtman N, Sima CS, Zakowski MF, Pao W, Kris MG, Miller VA, Ladanyi M and Riely GJ: Analysis of tumor specimens at the time of acquired resistance to EGFR-TKI therapy in 155 patients with EGFR-mutant lung cancers. *Clin Cancer Res* 19: 2240-2247, 2013.
8. Ku BM, Bae YH, Koh J, Sun JM, Lee SH, Ahn JS, Park K and Ahn MJ: AZD9291 overcomes T790 M-mediated resistance through degradation of EGFR(L858R/T790M) in non-small cell lung cancer cells. *Invest New Drugs* 34: 407-415, 2016.
9. Oxnard GR, Arcila ME, Sima CS, Riely GJ, Chmielecki J, Kris MG, Pao W, Ladanyi M and Miller VA: Acquired resistance to EGFR tyrosine kinase inhibitors in EGFR-mutant lung cancer: Distinct natural history of patients with tumors harboring the T790M mutation. *Clin Cancer Res* 17: 1616-1622, 2011.

10. Cross DA, Ashton SE, Ghiorghiu S, Eberlein C, Nebhan CA, Spitzler PJ, Orme JP, Finlay MR, Ward RA, Mellor MJ, *et al*: AZD9291, an irreversible EGFR TKI, overcomes T790M-mediated resistance to EGFR inhibitors in lung cancer. *Cancer Discov* 4: 1046-1061, 2014.
11. Finlay MR, Anderton M, Ashton S, Ballard P, Bethel PA, Box MR, Bradbury RH, Brown SJ, Butterworth S, Campbell A, *et al*: Discovery of a potent and selective EGFR inhibitor (AZD9291) of both sensitizing and T790M resistance mutations that spares the wild type form of the receptor. *J Med Chem* 57: 8249-8267, 2014.
12. FDA: FDA approves new pill to treat certain patients with non-small cell lung cancer, 2015. Available at Osimertinib in models of EGFR-mutant NSCLC brain metastases. <http://www.fda.gov/News/Events/Newsroom/PressAnnouncements/ucm472525.htm>. Accessed November 13, 2015.
13. Ramalingam SS, Reungwetwattana T and Chewaskulyong B: Osimertinib versus standard-of-care EGFR-TKI as first-line treatment in patients with EGFRm advanced NSCLC: FLARA. Presented at the ESMO Congress, Madrid, (abstract LBA2), 2017. <https://oncologypro.esmo.org/Meeting-Resources/ESMO-2017-Congress/Osimertinib-vs-standard-of-care-SoC-EGFR-TKI-as-first-line-therapy-in-patients-pts-with-EGFRm-advanced-NSCLC-FLAURA>.
14. Delaney G, Barton M, Jacob S and Jalaludin B: A model for decision making for the use of radiotherapy in lung cancer. *Lancet Oncol* 4: 120-128, 2003.
15. Bokobza SM, Jiang Y, Weber AM, Devery AM and Ryan AJ: Short-course treatment with gefitinib enhances curative potential of radiation therapy in a mouse model of human non-small cell lung cancer. *Int J Radiat Oncol Biol Phys* 88: 947-954, 2014.
16. Zhang S, Zheng X, Huang H, Wu K, Wang B, Chen X and Ma S: Afatinib increases sensitivity to radiation in non-small cell lung cancer cells with acquired EGFR T790M mutation. *Oncotarget* 6: 5832-5845, 2015.
17. Kriegs M, Gurtner K, Can Y, Brammer I, Rieckmann T, Oertel R, Wysocki M, Dorniock F, Gal A, Grob TJ, *et al*: Radiosensitization of NSCLC cells by EGFR inhibition is the result of an enhanced p53-dependent G1 arrest. *Radiother Oncol* 115: 120-127, 2015.
18. Ready N, Jänne PA, Bogart J, Dipetrillo T, Garst J, Graziano S, Gu L, Wang X, Green MR and Vokes EE; Cancer, Leukemia Group B, Chicago, IL: Chemoradiotherapy and gefitinib in stage III non-small cell lung cancer with epidermal growth factor receptor and KRAS mutation analysis: Cancer and leukemia group B (CALEB) 30106, a CALGB-stratified phase II trial. *J Thorac Oncol* 5: 1382-1390, 2010.
19. Kelly K, Chansky K, Gaspar LE, Albain KS, Jett J, Ung YC, Lau DH, Crowley JJ and Gandara DR: Phase III trial of maintenance gefitinib or placebo after concurrent chemoradiotherapy and docetaxel consolidation in inoperable stage III non-small-cell lung cancer: SWOG S0023. *J Clin Oncol* 26: 2450-2456, 2008.
20. Choong NW, Mauer AM, Haraf DJ, Lester E, Hoffman PC, Kozloff M, Lin S, Dancey JE, Szeto L, Grushko T, *et al*: Phase I trial of erlotinib-based multimodality therapy for inoperable stage III non-small cell lung cancer. *J Thorac Oncol* 3: 1003-1011, 2008.
21. Komaki R, Blumenschein GR, Wistuba II, Lee JJ, Allen P, Wei X, Welsh J, O'Reilly M, Herbst RS, Tang X, *et al*: Phase II trial of erlotinib and radiotherapy following chemoradiotherapy for patients with stage III non-small cell lung cancer. *J Clin Oncol* 29 (Suppl 15): 7020, 2011.
22. Kalvass JC, Maurer TS and Pollack GM: Use of plasma and brain unbound fractions to assess the extent of brain distribution of 34 drugs: Comparison of unbound concentration ratios to in vivo p-glycoprotein efflux ratios. *Drug Metab Dispos* 35: 660-666, 2007.
23. Casal Rubio J, Ffírvda-Pérez JL, Lázaro-Quintela M, Barón-Duarte FJ, Alonso-Jáudenes G, Santomé L, Afonso-Afonso FJ, Amenedo M, Huidobro G, Campos-Balea B, *et al*: A phase II trial of erlotinib as maintenance treatment after concurrent chemoradiotherapy in stage III non-small-cell lung cancer (NSCLC): A Galician Lung Cancer Group (GGCP) study. *Cancer Chemother Pharmacol* 73: 451-457, 2014.
24. Sequist LV, Martins RG, Spigel D, Grunberg SM, Spira A, Jänne PA, Joshi VA, McCollum D, Evans TL, Muzikansky A, *et al*: First-line gefitinib in patients with advanced non-small-cell lung cancer harboring somatic EGFR mutations. *J Clin Oncol* 26: 2442-2449, 2008.
25. Xu Y, Zheng Y, Sun X, Yu X, Gu J, Wu W, Zhang G, Hu J, Sun W and Mao W: Concurrent radiotherapy with gefitinib in elderly patients with esophageal squamous cell carcinoma: Preliminary results of a phase II study. *Oncotarget* 6: 38429-38439, 2015.
26. Park SY, Kim YM and Pyo H: Gefitinib radiosensitizes non-small cell lung cancer cells through inhibition of ataxia telangiectasia mutated. *Mol Cancer* 9: 222, 2010.
27. Das AK, Sato M, Story MD, Peyton M, Graves R, Redpath S, Girard L, Gazdar AF, Shay JW, Minna JD, *et al*: Non-small-cell lung cancers with kinase domain mutations in the epidermal growth factor receptor are sensitive to ionizing radiation. *Cancer Res* 66: 9601-9608, 2006.
28. Das AK, Chen BP, Story MD, Sato M, Minna JD, Chen DJ and Nirodi CS: Somatic mutations in the tyrosine kinase domain of epidermal growth factor receptor (EGFR) abrogate EGFR-mediated radioprotection in non-small cell lung carcinoma. *Cancer Res* 67: 5267-5274, 2007.
29. Dittmann K, Mayer C, Fehrenbacher B, Schaller M, Kehlbach R and Rodemann HP: Nuclear EGFR shuttling induced by ionizing radiation is regulated by phosphorylation at residue Thr654. *FEBS Lett* 584: 3878-3884, 2010.
30. Dittmann K, Mayer C, Fehrenbacher B, Schaller M, Raju U, Milas L, Chen DJ, Kehlbach R and Rodemann HP: Radiation-induced epidermal growth factor receptor nuclear import is linked to activation of DNA-dependent protein kinase. *J Biol Chem* 280: 31182-31189, 2005.
31. Toulany M, Kasten-Pisula U, Brammer I, Wang S, Chen J, Dittmann K, Baumann M, Dikomey E and Rodemann HP: Blockage of epidermal growth factor receptor-phosphatidylinositol 3-kinase-AKT signaling increases radiosensitivity of K-RAS mutated human tumor cells in vitro by affecting DNA repair. *Clin Cancer Res* 12: 4119-4126, 2006.
32. Rodemann HP, Dittmann K and Toulany M: Radiation-induced EGFR-signaling and control of DNA-damage repair. *Int J Radiat Biol* 83: 781-791, 2007.
33. Kriegs M, Kasten-Pisula U, Rieckmann T, Holst K, Saker J, Dahm-Daphi J and Dikomey E: The epidermal growth factor receptor modulates DNA double-strand break repair by regulating non-homologous end-joining. *DNA Repair (Amst)* 9: 889-897, 2010.
34. Myllynen L, Rieckmann T, Dahm-Daphi J, Kasten-Pisula U, Petersen C, Dikomey E and Kriegs M: In tumor cells regulation of DNA double strand break repair through EGF receptor involves both NHEJ and HR and is independent of p53 and K-Ras status. *Radiother Oncol* 101: 147-151, 2011.
35. Löbrich M, Shibata A, Beucher A, Fisher A, Ensminger M, Goodarzi AA, Barton O and Jeggo PA: gammaH2AX foci analysis for monitoring DNA double-strand break repair: Strengths, limitations and optimization. *Cell Cycle* 9: 662-669, 2010.
36. Lord CJ and Ashworth A: The DNA damage response and cancer therapy. *Nature* 481: 287-294, 2012.
37. Li B, Yuan M, Kim IA, Chang CM, Bernhard EJ and Shu HK: Mutant epidermal growth factor receptor displays increased signaling through the phosphatidylinositol-3 kinase/AKT pathway and promotes radioresistance in cells of astrocytic origin. *Oncogene* 23: 4594-4602, 2004.
38. Sun Y, Moretti L, Giacalone NJ, Schleicher S, Speirs CK, Carbone DP and Lu B: Inhibition of JAK2 signaling by TG101209 enhances radiotherapy in lung cancer models. *J Thorac Oncol* 6: 699-706, 2011.
39. Dent P, Yacoub A, Contessa J, Caron R, Amorino G, Valerie K, Hagan MP, Grant S and Schmidt-Ullrich R: Stress and radiation-induced activation of multiple intracellular signaling pathways. *Radiat Res* 159: 283-300, 2003.
40. Walter AO, Sjin RT, Haringsma HJ, Ohashi K, Sun J, Lee K, Dubrovskiy A, Labenski M, Zhu Z, Wang Z, *et al*: Discovery of a mutant-selective covalent inhibitor of EGFR that overcomes T790M-mediated resistance in NSCLC. *Cancer Discov* 3: 1404-1415, 2013.
41. Ercan D, Xu C, Yanagita M, Monast CS, Pratilas CA, Montero J, Butaney M, Shimamura T, Sholl L, Ivanova EV, *et al*: Reactivation of ERK signaling causes resistance to EGFR kinase inhibitors. *Cancer Discov* 2: 934-947, 2012.
42. Cortot AB, Repellin CE, Shimamura T, Capelletti M, Zejnullahu K, Ercan D, Christensen JG, Wong KK, Gray NS and Jänne PA: Resistance to irreversible EGF receptor tyrosine kinase inhibitors through a multistep mechanism involving the IGF1R pathway. *Cancer Res* 73: 834-843, 2013.



This work is licensed under a Creative Commons Attribution-NonCommercial-NoDerivatives 4.0 International (CC BY-NC-ND 4.0) License.